RGS4 inhibits angiotensin II signaling and macrophage localization during renal reperfusion injury independent of vasospasm

Paul Pang[1], Xiaohua Jin[2], Brandon M. Proctor[2], Michelle Farley[3], Nilay Roy[4], Matthew S. Chin[5], Ulrich H. von Andrian[6,7], Elisabeth Vollmann[6], Mario Perro[6], Ryan J. Hoffman[8], Joseph Chung[1], Nikita Chauhan[1], Murti Mistri[1], Anthony J. Muslin[2], Joseph V. Bonventre[1] and Andrew M. Siedlecki[1]

[1]Renal Division, Department of Internal Medicine, Brigham and Women's Hospital, Harvard Medical School, Harvard Institutes of Medicine, Boston, Massachusetts, USA; [2]Washington University in St Louis School of Medicine, St Louis, Missouri, USA; [3]Beth Israel Deaconess Medical Center, Boston, Massachusetts, USA; [4]Partners Healthcare, Boston, Massachusetts, USA; [5]University of North Carolina School of Medicine, Chapel Hill, North Carolina, USA; [6]Harvard Medical School, Boston, Massachusetts, USA; [7]Ragon Institute of Massachusetts General Hospital, Massachusetts Institute of Technology, Harvard University, Cambridge, Massachusetts, USA and [8]Wesleyan University, Middletown, Connecticut, USA

Vascular inflammation is a major contributor to the severity of acute kidney injury. In the context of vasospasm-independent reperfusion injury we studied the potential anti-inflammatory role of the Gα-related RGS protein, RGS4. Transgenic RGS4 mice were resistant to 25 min injury, although post-ischemic renal arteriolar diameter was equal to the wild type early after injury. A 10 min unilateral injury was performed to study reperfusion without vasospasm. Eighteen hours after injury, blood flow was decreased in the inner cortex of wild-type mice with preservation of tubular architecture. Angiotensin II levels in the kidneys of wild-type and transgenic mice were elevated in a sub-vasoconstrictive range 12 and 18 h after injury. Angiotensin II stimulated pre-glomerular vascular smooth muscle cells (VSMCs) to secrete the macrophage chemoattractant RANTES, a process decreased by angiotensin II R2 (AT2) inhibition. However, RANTES increased when RGS4 expression was suppressed implicating Gα protein activation in an AT2-RGS4-dependent pathway. RGS4 function, specific to VSMC, was tested in a conditional VSMC-specific RGS4 knockout showing high macrophage density by T2 MRI compared with transgenic and non-transgenic mice after the 10 min injury. Arteriolar diameter of this knockout was unchanged at successive time points after injury. Thus, RGS4 expression, specific to renal VSMC, inhibits angiotensin II-mediated cytokine signaling and macrophage recruitment during reperfusion, distinct from vasomotor regulation.

Kidney International (2015) **87,** 771–783; doi:10.1038/ki.2014.364; published online 3 December 2014

Correspondence: *Andrew M. Siedlecki, Renal Division, Department of Internal Medicine, Brigham and Women's Hospital, Harvard Medical School, Harvard Institutes of Medicine, 77 Avenue Louis Pasteur, Boston, Massachusetts, 02115. E-mail: asiedlecki@partners.org*

Received 21 May 2014; revised 3 September 2014; accepted 11 September 2014; published online 3 December 2014

KEYWORDS: acute kidney injury; ischemia reperfusion; renin angiotensin system

Regulators of G protein signaling (RGS) proteins are key components in the vascular function of the kidney.[1,2] They have also been attributed anti-inflammatory properties in disease states such as atherosclerosis and diabetic cardiomyopathy.[3–5] The RGSare GTPase activating proteins that bind to heterotrimeric Gαβγ proteins and inactivate the α subunit. RGS4 is subcategorized as a vascular-associated RGS protein with GTPase activating protein function for Gq and Gi family members.[6,7] In addition to modulating vascular tone,[2] RGS4 is upregulated in vascular smooth muscle cells (VSMCs) susceptible to atherosclerosis.[3] RGS4 also contributes to a decrease in angiotensin-dependent superoxide production,[8] prevents vascular oxidation,[5] and may be involved in the inhibition of cell signaling through CXC-motif chemokine receptors.[9]

The alpha subunit in Gα-containing receptors (GαRs) is a well-known RGS4 binding partner.[10] We have previously shown RGS4 to inactivate the endothelin-1, Gα- associated, receptor in the kidney. In the absence of RGS4, acute ischemic injury is prolonged. However, the activity of RGS4 on angiotensin-II (AngII) signaling in the context of reperfusion is unclear. AngII can activate local cytokine signaling in the VSMC,[11] initiate TGF-β signaling in tubular epithelial cells,[12] provoke activation of the coagulation cascade on the surface of the endothelial cell,[13] induce leukocyte adhesion in arterioles[14,] and induce endothelial cell senescence[15] independent of its vasconstrictive action.

Activation of G protein–coupled receptors in the renal microvasculature by endothelin-1 and AngII is central to the progress of ischemia/reperfusion injury (IRI).[16–19] AngII generation is stimulated by hypoperfusion initially but may

be perpetuated by endothelial injury and localized production of angiotensin converting enzyme in monocytes[20] independent of ischemic conditions. In turn it has been recognized that leukocyte binding in the renal microvasculature during reperfusion is not dependent on arterial vasoconstriction.[21] By discriminating between the vasoactive and non-vasoactive effect of RGS4-monitored G protein–coupled receptor signaling, one can better understand the inciting events leading to microvasculature injury in the kidney. Contrasting our earlier work, which focused on the ischemic component of IRI, we report on the anti-inflammatory function of RGS4 that is distinct from the modulation of arterial vasoconstriction. By specifically enhancing RGS4 expression in an animal model, we demonstrate that RGS4 is a critical agent in the prevention of reperfusion injury.

RESULTS

Enhanced RGS4 expression in the microvasculature prevents acute kidney injury

RGS4 expression has been identified in arteries of the kidney with a β-galactosidase (βgal) gene knock-in reporter system (RGS4 LacZ).[2] We compared the RGS4 LacZ RGS4 reporter system with a second model that incorporates multiple copies of a bacterial artificial chromosome. The RGS4 LacZ construct has been described previously. The bacterial artificial chromosome transgene contains the RGS4 coding region and an IRES-eGFP construct inserted into the 3′ UTR of the RGS4 locus.[22,23] We further used the RGS4-eGFP transgenic mouse (Tg) as a relative overexpressor[22] to contrast our previous description of the *rgs4*-null mouse.[2,24]

At baseline, RGS4-promoter-driven βgal in the RGS4 LacZ is expressed in afferent and efferent arterioles (Figure 1a) and peritubular capillaries. In Tg animals, RGS4 co-localizes with smooth muscle myosin heavy chain positive (MHC+) cells in the kidney consistent with small vascular structures of the inner cortex and outer medulla (Figure 1b). This was demonstrated by histology and quantified by FACS analysis where RGS4+ cells were found to be a subset of SMMHC+ cells (Figure 1c).

Four hours after the initiation of kidney reperfusion, the endogenous RGS4 promoter was more readily bound by RNA polymerase and tissue levels of RGS4 protein increased. Binding of the RGS4 promoter resulting in RGS4 mRNA transcription is directly correlated to βgal expression in the RGS4 LacZ animal model as previously reported.[7] Congenic controls displayed an increased amount of RGS4 protein in kidney tissue at the same 4-h time point (Figure 2a and b). RGS4 protein levels rapidly declined at later time points in wild-type (WT) animals. This was consistent with βgal expression in the corticomedullary junction of RGS4 LacZ animals (Figure 2a) and with RGS4 protein levels in the same

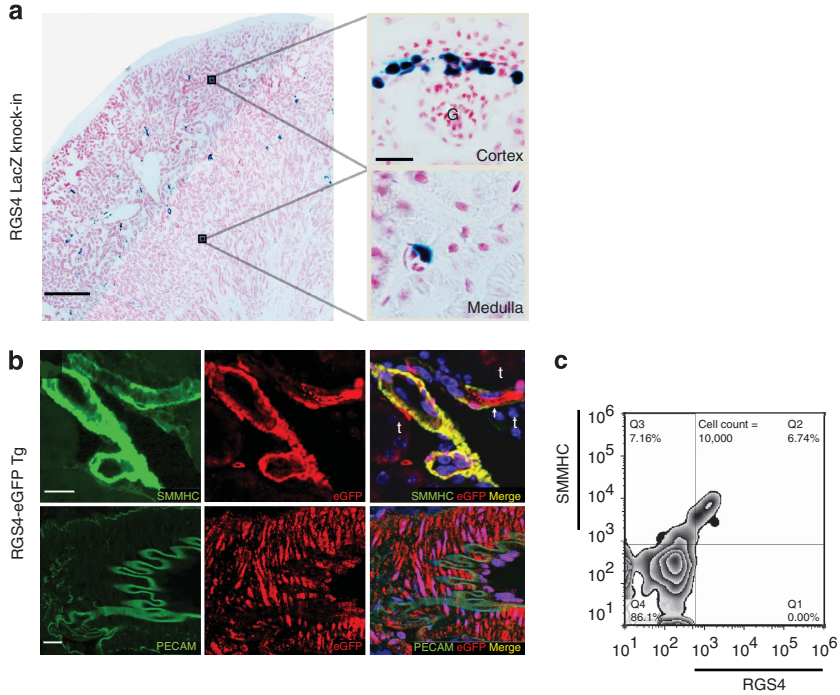

Figure 1 | Regulators of G protein signaling 4 (RGS4) expression in the kidney of β-galactosidase (β-gal) knock-in and eGFP transgenic reporter systems. (**a**) Composite images were analyzed for baseline RGS4-driven β-gal expression (scale bar = 500 μm). β-Gal is expressed in the outer cortex of the afferent and efferent arterioles of glomeruli (G) and in peritubular capillaries (scale bar = 25 μm). (**b**) RGS4 expression in the eGFP transgenic reporter system is present in arterioles and capillaries adjacent to tubules (t) (top row) (scale bar = 25 μm). Midsized vessels express RGS4 in SMMHC+ cells in the medial wall adjacent to PECAM+ cells in the intimal lining (bottom row) with no apparent co-localization (scale bar = 25 μm). (**c**) Flow cytometry of kidney digest from transgenic (Tg), first permeabilized then probed with monoclonal antibodies to SMMHC and RGS4. 48.5% ± 3.2 of SMMHC+ cells were also RGS4+/SMMHC+ ($n = 4$). SMMHC, smooth muscle myosin heavy chain.

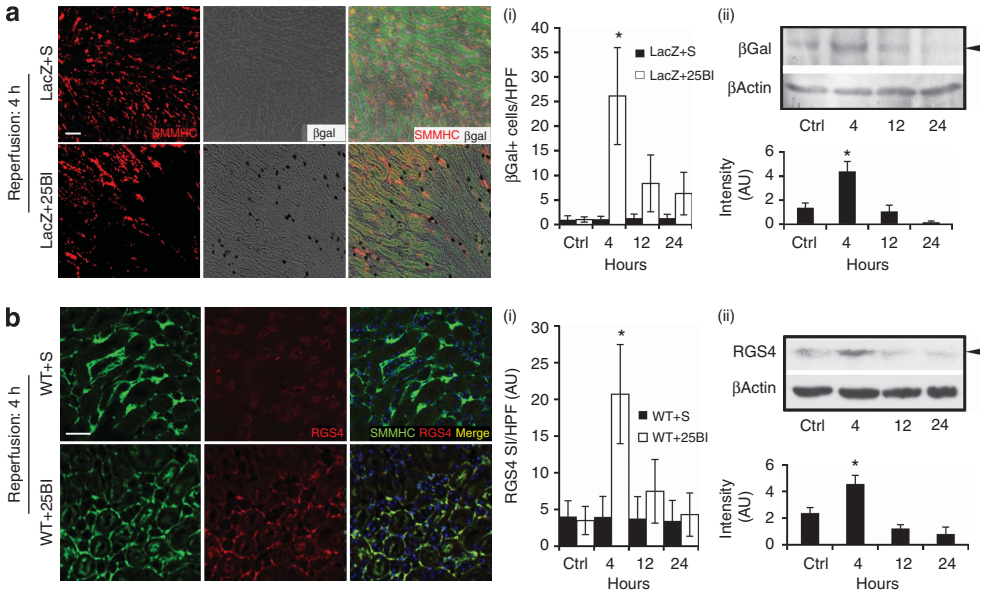

Figure 2 | Regulators of G protein signaling 4 (RGS4) expression in renal tissue before and after standard ischemic injury and RGS4 overexpression. (**a**) RGS4-LacZ reporter mice express SMMHC (red) consistent with typical histologic location of microvasculature adjacent to epithelial tubular cells (green epifluorescence) in animals undergoing sham ischemic kidney injury (scale bar = 50 μm) (top row). (i) RGS4-LacZ animals express β-galactosidase (black, bright field) after 25 min bilateral injury (LacZ + 25 min bilateral ischemic injury (25BI)) (26 ± 10cells/hpf) ($n = 10$) most accentuated 4 h after ischemia (bottom row) compared with 12 h (8 ± 6) ($n = 9$), ($^*P = 3.4 \times 10^{-10}$). (ii) Representative luminescent intensity in arbitrary units (AUs) from an immunoblot of RGS4-LacZ kidney tissue after 25BI, probed with anti-beta galactosidase (βgal) antibody and developed with horseradish peroxidase ($n = 6,6,6,6$ per group) control (1.37 ± 0.39) versus 4 h after ischemia (4.38 ± 0.81) ($^*P = 0.01$). (**b**) A similar expression pattern is identified in non-transgenic animals analyzed with anti-RGS4 monoclonal antibody (red). (i) RGS4-specific binding was quantified by cy3 signal intensity per high power field (SI/HPF). Structures consistent with arterioles and peritubular capillaries contained both SMMHC and RGS4 in shams (top row) and 4 h after 25BI (bottom row) (scale bar = 50 μm). Wild type (WT) + 25BI at 4 h (20.7 ± 6.7) ($n = 8$) vs. 12 h (7.5 ± 4.3) ($n = 8$), ($^*P = 1.8 \times 10^{-9}$). (ii) Representative luminescent intensity in AUs from an immunoblot of RGS4 in WT kidney tissue after 25 min ischemic injury, probed with anti-RGS4 monoclonal antibody and developed with horseradish peroxidase ($n = 8,8,8,8$ per group) control (2.39 ± 0.4) vs. 4 h after ischemia (4.56 ± 0.65) ($^*P = 0.002$).

region of WT (Figure 2b). We therefore hypothesized that increased RGS4 protein expression in the kidneys of Tg mice is protective in the setting of ischemia-reperfusion injury and contrasts the phenotype of *rgs4*-null mice.[2] After 25 min bilateral ischemic injury (25BI), renal function in Tg was preserved in comparison to littermate controls (Figure 3a) and corresponded with a reduction in tubular injury after 24 h (Figure 3b) when Tg animals expressed maintained levels of RGS4 compared with WT + IRI (Figure 3c).

RGS4 prevents reperfusion injury in a non-vasoconstricted state

Experiments above showed that RGS4 is expressed in VSMCs of the kidney. Although we also observed baseline blood pressure in Tg animals equivalent to congenic controls (Supplementary Figure S1 online), we had previously described prolonged vasospasm in *rgs4*-null mice after endothelin-1 challenge.[2] We therefore evaluated whether the preservation of renal function in RGS4 transgenic mice was due to an abrogation of vasospasm. We tested this hypothesis by performing a series of experiments involving *in vivo* 2-photon microscopy. Unexpectedly, we found after 25BI, cross-sectional renal arteriolar diameter of injured Tg was equivalent to injured WT after 0.5, 1, 6, 18, and 24 h (Figure 4a). Because RGS4 has been independently associated with the modulation of macrophage transit[3,4] we probed tissue with ED1 monoclonal antibody. ED1 + cell density was decreased in Tg animals compared with injured controls 18 h after 25BI (Figure 4b). These results left the etiology of the RGS4 renoprotective effect unresolved as vasomodulatory or immunomodulatory in nature. To isolate the influence of VSMC in the microvasculature without implicating prolonged vasospasm and the sequela of tubular injury, we performed a 10-minunilateral ischemia (10UI) and evaluated vasoactive parameters at late successive time points in the injured kidney. Tubular injury scores indicated no presence of acute tubular necrosis 18 h after microvascular clamp release (data not shown). Immunohistologic probe for KIM-1, a sensitive biomarker of tubular epithelial injury, was not detected in a density greater than shams (Figure 5a and b). *In vivo* renal arteriolar diameters in Tg + 10UI and WT + 10UI were unchanged after 0.5, 1, 6, 18, and 24 h of reperfusion compared with no injury (Figure 5c).

Eighteen hours after 10UI, we evaluated *in vivo* renal blood flow by MRI. Fast imaging with steady-state precession is a form of dynamic magnetic resonance imaging capable of measuring small alterations in blood flow. We adapted fast imaging with steady-state precession MR imaging techniques

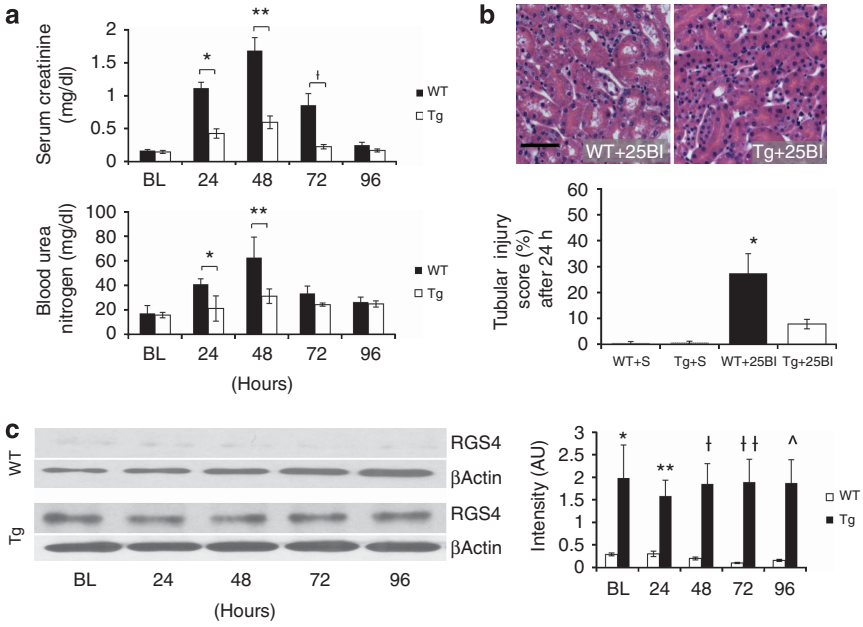

Figure 3 | Regulators of G protein signaling 4 (RGS4) overexpression prevents acute kidney injury. (**a**) Twenty-four hours after injury, blood urea nitrogen (BUN) (mg/dl) in control ($n=6$) animals increased to 40.9 ± 4. vs. 31.1 ± 6.0 in transgenic (Tg; $n=6$) (*$P=0.004$); after 48 h, 62.6 ± 16.8 ($n=6$) vs. 31.1 ± 6.0 ($n=6$), respectively (**$P=2.56\times10^{-5}$); after 72 h, 33.4 ± 6.0 ($n=6$) vs. 24.3 ± 1.3 ($n=6$) ($P=$NS). Twenty-four hours after injury, serum creatinine (sCr, mg/dl) in control animals increased to 1.12 ± 0.09 ($n=6$) vs. Tg 0.43 ± 0.07 ($n=6$)(*$P=6.26\times10^{-5}$); after 48 h, 1.68 ± 0.20 ($n=6$) vs. 0.60 ± 0.10 ($n=6$), respectively (**$P=5.09\times10^{-10}$); after 72 h, 0.85 ± 0.18 ($n=6$) vs. 0.24 ± 0.03 ($n=6$), respectively ($^{\dagger}P=0.004$); after 96 h, 0.25 ± 0.04 vs. 0.17 ± 0.07 ($P=$NS). (**b**) Kidney tissue from littermate controls and Tg animals was stained with hematoxylin and eosin to evaluate cellular structures for damage. To calculate a tubular injury score, kidney sections were processed after 24 h of reperfusion and were evaluated for tubule flattening, necrosis, apoptosis, or the presence of casts as a percentage of total number of tubular epithelial cells per high power field. Wild type (WT) + 25 min bilateral ischemic injury (25BI) (27.8 ± 8.3%) ($n=7$) vs. Tg + 25BI (8.2 ± 2.4%) ($n=7$), (*$P=0.002$) (scale bar = 50 μm). (**c**) RGS4 protein levels were measured by immunoblot technique at corresponding time points after injury in wild-type controls and RGS4 overexpressor animals, (Tg) respectively, at baseline (0.286 ± 0.032 ($n=8$) vs. 1.98 ± 0.736 ($n=8$) (*$P=1.94\times10^{-9}$)), at 24 h (0.298 ± 0.0613 ($n=8$) vs. 1.58 ± 0.353 ($n=8$), (**$P=2.42\times10^{-9}$)), at 48 h (0.196 ± 0.031 ($n=8$) vs. 1.85 ± 0.451 ($n=8$), ($^{\dagger}P=4.93\times10^{-13}$)), at 72 h (0.0964 ± 0.0123 ($n=8$) vs. 1.89 ± 0.509 ($n=8$), ($^{\dagger\dagger}P=2.59\times10^{-14}$)), and at 96 h (0.153 ± 0.0241 ($n=8$) vs. 1.87 ± 0.518 ($n=8$), (^$P=1.17\times10^{-13}$)).

to analyze *in vivo* renal blood flow (Figure 5d). The use of local arterial input function avoided the need for deconvolution of a global arterial input function (see Materials and Methods). Rate change of contrast inflow (α) correlated closely with rate change of contrast outflow (β), whereas renal blood flow measures did not correlate directly with either α or β (Supplementary Figure S2 online). Small regions of interest were analyzed with a computational algorithm using Bayesian analytic techniques,[25] which demonstrated a difference in blood flow most apparent at the junction of the inner cortex and outer medulla (Supplementary movies 1–3). We observed a reduction in flow after 18 h of reperfusion in littermate controls, whereas Tg animals maintained perfusion equivalent to those observed in shams (Figure 5e). The disturbance in blood flow occurred in conditions where renal microvascular cross-sectional area, tubular injury scores, and KIM-1 expression were equivalent to shams.

RGS4 inhibits Ang-II-dependent RANTES synthesis in human aorta-derived VSMC

AngII may contribute to reperfusion injury through activation of Gα-containing AngII receptors without affecting vasomotor tone.[14] *Ex vivo* kidneys were prepared[2] from littermate controls and Tg animals as we previously described. Kidneys were perfused with 10 pg/min of AngII. Rate change in pressure per unit time ($+\Delta p/\Delta t$) after 40 pg/min of AngII for 20 min in isolated WT kidneys was 1.55 mm Hg ($n=6$) versus no change in WT infused with 10 pg/min ($n=6$). $+\Delta p/\Delta t$ in Tg infused with 40 pg/min of AngII ($n=6$) was 1.33 mm Hg versus no change in Tg infused with 10 pg/min ($n=6$) (Figure 6a). Hence, there was no increase in perfusion pressure at the lower dose of AngII, but *ex vivo* kidney tissue levels were comparable to elevated tissue levels from kidneys procured after 12 and 18 h of reperfusion post 10UI (Figure 6b).

We evaluated possible cytokine signals that could be modulated by VSMC-dependent RGS4 expression. Primary human arterial VSMC cells were cultured and stimulated with AngII. VSMC supernatant was screened for 18 signaling cytokines (Figure 7a). Regulated and normal t cell expressed and secreted (RANTES), a monocyte chemoattractant secreted by VSMCs,[26] was elevated. Other cytokines known to be expressed by VSMCs were also detected including MCP-1, IP-10, and VEGF. Levels of RANTES increased in response to AngII in a time-dependent manner (Figure 7a

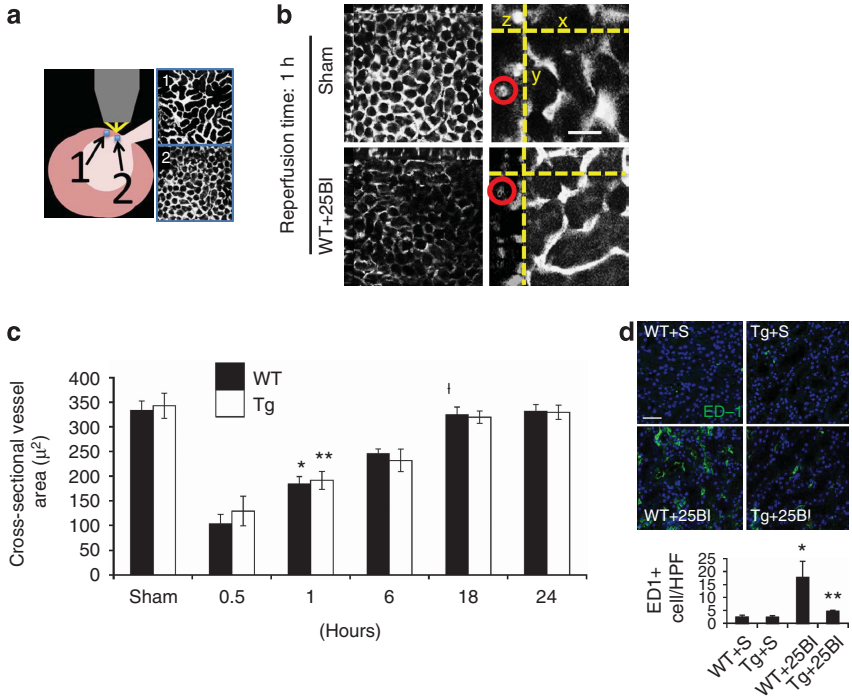

Figure 4 | Small renal vessel response to reperfusion in regulators of G protein signaling 4 (RGS4) transgenic (Tg) after 25 min bilateral ischemic injury (25BI). (**a**) Cutaneous regions proximate to the hilum exposed a confluence of (1) superficial cortical and (2) deeper structures. (**b**) Real-time small vessel diameter (red circle) from regions representative of deep kidney structures was measured with 2-photon microscopy (low power, left panels; high power, right panels, scale bar = 60 μm). Three-dimensional images were re-constructed at successive time points after 25 min bilateral renal microvascular clamp injury. (**c**) Cross-sectional areas of vessels (μm^2) of wild-type versus RGS4 transgenic animals were compared at baseline ($n = 4$ animals per group) (324 ± 21 vs. 339 ± 17), 0.5 h (104 ± 19 vs. 122 ± 17), 1 h (179 ± 21 vs. 186 ± 21), 6 h (242 ± 18 vs. 230 ± 16), 18 h (321 ± 20 vs. 322 ± 19), and 24 h (329 ± 17 vs. 326 ± 18), respectively. Wild type (WT) 0.5 h vs. WT 1 h, $^{*}P = 3.9\times10^{-7}$; Tg 0.5 h vs. Tg 1 h, $^{**}P = 3.8\times10^{-6}$. (**d**) Eighteen hours after bilateral microvascular clamps were released, kidney tissue was procured from RGS4 transgenics and wild-type controls. Frozen sections were probed with ED1 monoclonal antibody, WT + S (2.5 ± 0.7 cells/hpf) ($n = 5$) vs. WT + 25BI (17.8 ± 6.1) ($n = 6$), $^{*}P = 4.8\times10^{-5}$; Tg + 25BI (4.7 ± 0.4) ($n = 6$) vs. WT + 25BI, $^{**}P = 6.1\times10^{-10}$ (scale bar = 50 μm).

inset). Secretion was exacerbated by RGS4 knockdown and was inhibited by pretreatment with PD123319 (1 μmol/l), a specific inhibitor of the AngII type 2 receptor. Pretreatment with losartan (1 μmol/l) had no antagonistic effect (Figure 7b).

Murine pre-glomerular vascular smooth muscle cells (PGVSMCs) were then interrogated to determine whether RANTES expression was modified by RGS4 expression in the above animal models. Isolation of PGVSMC was performed using an established technique.[27] In brief, intra-arterial injection of iron oxide nanoparticles allowed for isolation of pre-glomerular arterioles by positive paramagnetic selection. Intact microvascular structures were then exposed to escalating doses of AngII. Vessel diameter was unchanged at low concentrations (1×10^{-9}mol/l) (Figure 7c). PGVSMCs were also isolated and cultured. After exposure to AngII (1×10^{-9}mol/l), RANTES levels in the supernatant were elevated 125% in WT (6.3 ± 1.0 pg/ml) compared with R4Tg-derived (2.8 ± 1.0)($P = 1.4\times10^{-6}$) (Figure 7d). RANTES levels were also elevated in WT compared with R4Tg after exposure to 1×10^{-8}mol/l and 1×10^{-7}mol/l AngII.

RGS4 expressed in SMMHC + cells in the kidney compartment protects against macrophage localization in reperfusion injury

To determine the isolated function of RGS4 in VSMCs in an animal model, we employed a VSMC–specific, RGS4 knockout animal model. A conditional RGS4-null mouse was created using a smooth muscle cell myosin heavy chain-11 (SMHHC) promoter to drive expression of Cre recombinase.[28] The myosin heavy chain-11 promoter was used to select for differentiated cells with contractile function, avoiding Cre expression in poorly differentiated fibroblasts or myofibroblasts.[29,30] The SMMHC-Cre animal was crossed to the floxed animal, *rgs4*$^{fl/fl}$, generating a conditional knockout mouse, SMHHC-Cre *rgs4*$^{fl/fl}$ (CKO) (Figure 8). Cumulative survival after 25BI was decreased compared with SMMHC-Cre (Cre) controls undergoing the same 25BI procedure (Figure 9a). Twenty-four hours after 25BI, CKO tubular injury scores were elevated compared with Cre controls undergoing 25BI (Figure 9b). Forty-eight hours after 25BI, CKO serum creatinine was elevated 88% greater than Cre controls undergoing 25BI (Figure 9c). However, after 10UI, *in vivo* cross-sectional arteriolar diameter of the injured

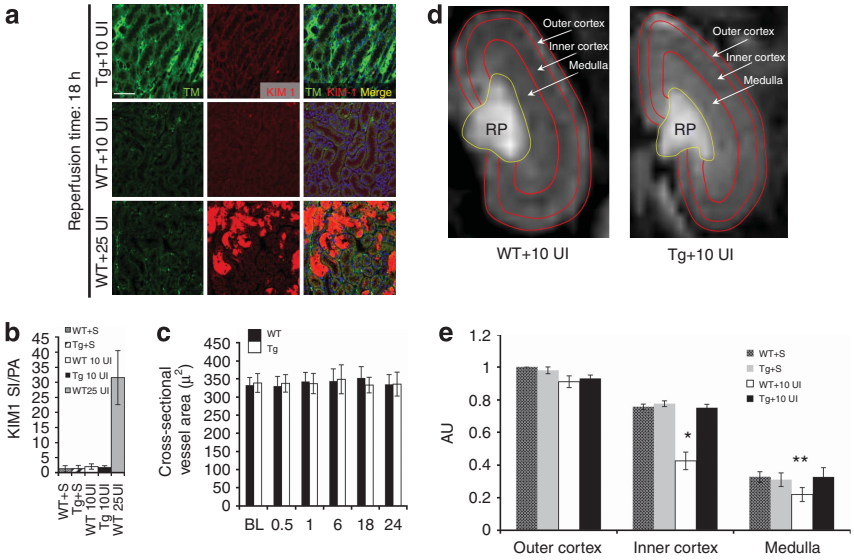

Figure 5 | Vascular changes after 10 min unilateral microvascular clamping. (**a**) Kidney tissue from wild-type mice 18 h after 10 min unilateral ischemia (10UI) and 25 min bilateral ischemic injury (25BI) probed for thrombomodulin and KIM-1 (scale bar = 100 μm). (**b**) Signal intensity (SI) (red) was normalized to pixel area (PA) per condition ($n = 5$ per group) (*$P < 0.001$, 25BI vs. Wild type (WT) 10UI). (**c**) Small vessel diameter (μm^2) by 2-photon microscopy in kidneys of WT and transgenic (Tg), respectively, undergoing 10UI, at baseline (BL) (332 ± 21 ($n = 6$) vs. 338 ± 26 ($n = 6$)), 0.5 h (329 ± 24 ($n = 6$) vs. 337 ± 24 ($n = 6$)), 1 h 342 ± 25 ($n = 6$) vs. 336 ± 28 ($n = 6$)), 1 h (342 ± 25 ($n = 6$) vs. 336 ± 28 ($n = 6$)), 6 h (343 ± 34 ($n = 6$) vs. 348 ± 41 ($n = 6$)), 18 h (352 ± 31 ($n = 6$) vs. 333 ± 22 ($n = 6$)), and 24 h (334 ± 27 ($n = 6$) vs. 335 ± 32 ($n = 6$)). (**d**) Dynamic MR imaging of the kidney after 10UI. Kidney distribution of gadolinium contrast 18 h after 10UI in regulators of G protein signaling 4 (RGS4) Tg (first window) and wild type (second window). Blood flow was measured by change in gadolinium contrast intensity in individual pixel areas of the outer cortex (OC), inner cortex (IC), and medulla (M) in the coronal plane. (**e**) Regional perfusion in RGS4 overexpressor (Tg)($n = 5$) was compared with matched littermate shams (WT)($n = 5$) 18 h after reperfusion. IC perfusion, WT + 10UI (0.24 ± 0.6) vs. Tg + 10UI (0.75 ± 0.04), (*$P = 2.4 \times 10^{-14}$), and medullary perfusion, WT + 10UI (0.22 ± 0.04) vs. Tg + 10UI (0.33 ± 0.06), (**$P = 0.002$).

kidney was unchanged compared with SMMHC-Cre controls (Figure 9d). *Ex vivo* CKO kidneys responded similarly to SMMHC-Cre and Tg animals after AngII infusion. Kidneys from CKO animals placed on perfusion apparatus were infused with 40 pg/min for 10 min with sustained change in pressure per unit time ($+\Delta p/\Delta t$): 1.47 mm Hg after 20 min ($P < 0.001$) versus no change in CKO infused with 10 pg/min (Figure 9e). Kidneys perfused with AngII at a rate of 10 pg/min contained elevated levels of tissue AngII similar to that found at the 12 and 18 h reperfusion time points after 10UI (Figure 9f).

We inferred that RGS4 depletion in VSMC would exacerbate AngII-induced monocyte localization because of the above findings including decreased ED1 + cell density in RGS4 overexpressors and RGS4-dependent modulation of RANTES secretion. Therefore, we injected monocrystalline iron oxide nanoparticles (MION-47) intravenously to localize phagocytic cells, primarily macrophages,[31] in live animals. Using 10 min unilateral kidney injury (10UI), we then measured macrophage localization in the late reperfusion period (i.e. 18 h of reperfusion). *In vivo* MR imaging of the injured kidney identified nanoparticles in CKO kidneys 18 h after 10UI. Particle density was greater in CKO kidneys after 10UI compared with Cre controls undergoing the same procedure (Figure 10a). Injured Tg animals had less nanoparticle density compared with injured Cre controls (Figure 10b). CKO animals treated with PD123319 followed by 10UI had reduced nanoparticle density approaching that of Tg + 10UI (Figure 10b). Increased density of ED1 + cells (Figure 11a and c) and Prussian blue + cells (Figure 11b and c) was coincident with a shorter normalized T2 relaxation time in CKO (Figure 10b). ED1 probing and Prussian blue staining were also decreased in CKO treated with PD123319.

DISCUSSION

On the basis of the above studies, we identify a previously unknown anti-inflammatory function of VSMCs in late reperfusion injury of the kidney. In particular, expression of RGS4 in smooth muscle cell–containing microvasculature decreases inflammatory signals that are transmitted by AngII receptor activation. We found that RGS4-overexpressing animals were protected from 25 min bilateral ischemic injury, as on the basis of serum creatinine values and tubular injury scoring. Our earlier work showed that the RGS4 global knockout was sensitive to renal IRI; therefore, the phenotype of the RGS4 overexpressor was not unexpected. However, it was unclear whether protection offered by RGS4 overexpression was exclusively due to vasoconstrictor blockade in this standard model. We observed RGS4 protein levels to be highest 4 h after microvascular clamp removal in 25 min bilateral ischemic renal injury, whereas tissue AngII levels remained elevated for several hours afterward. Takata *et al.*[3] showed that 2.5 μg/kg infusion of AngII over 4 weeks

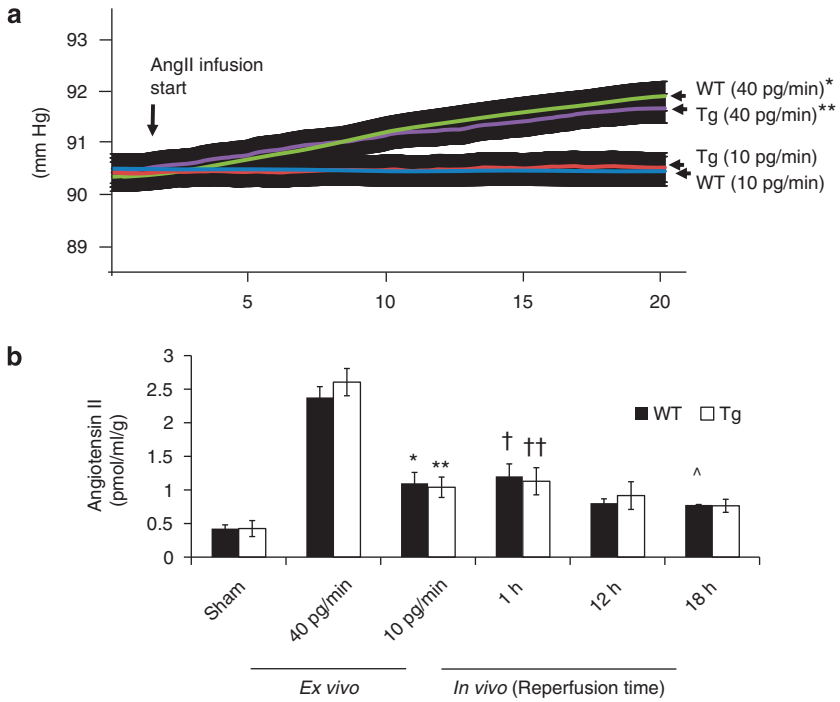

Figure 6 | Angiotensin II tissue levels increase after *ex vivo* angiotensin-II (AngII) infusion in a sub-vasoconstrictive range and after 10 min unilateral microvascular clamping. (**a**) Kidneys were isolated from wild-type (WT) or regulators of G protein signaling 4 (RGS4) transgenic overexpressor (TG) and placed on a perfusion apparatus and infused with 40 pg/min for 20 min. Baseline WT perfusion pressure 90.36 ± 0.44 ($n = 6$) vs. 91.94 ± 0.43 ($n = 6$) after WT, 20 min of AngII infusion, 40 pg/min ($^{*}P = 2.3\times10^{-7}$) vs. 20 min of AngII infusion, 10 pg/min, 90.39 ± 0.23 mm Hg ($n = 6$) (P = NS). Baseline Tg perfusion pressure (mm Hg) 90.47 ± 0.38 ($n = 6$) vs. 91.77 ± 0.39 ($n = 6$) after 20 min of AngII infusion, 40 pg/min ($^{**}P = 8.7\times10^{-7}$), vs. 20 min of AngII infusion, 10 pg/min, 90.44 ± 0.38 mm Hg ($n = 6$) (P = NS). (**b**) Injured kidneys were procured after 1, 12, and 18 h of reperfusion subsequent to 10 min unilateral microvascular clamping. AngII kidney tissue (g) levels (pmol/ml per g of kidney) in WT baseline (BL) (0.43 ± 0.05) ($n = 6$) vs. WT 10 pg/min (1.10 ± 0.16) ($n = 6$), ($^{*}P = 5.1\times10^{-5}$); Tg BL (0.43 ± 0.08) ($n = 6$) vs. Tg 10 pg/min (1.04 ± 0.15) ($n = 6$), ($^{**}P = 4.5\times10^{-5}$); WT 40 pg/min (2.38 ± 0.16) ($n = 6$) vs. WT 1 h post injury (1.20 ± 0.19) ($n = 6$), ($^{\dagger}P = 1.46\times10^{-8}$); Tg 40 pg/min (2.61 ± 0.20) ($n = 6$) vs. Tg 1 h post injury (1.13 ± 0.20) ($n = 6$), ($^{\dagger\dagger}P = 1.57\times10^{-8}$); WT12 h post injury (0.80 ± 0.06) ($n = 6$) vs. WT 10 pg/min (NS); Tg (0.92 ± 0.21) ($n = 6$) vs. TG 10 pg/min (NS); WT 18 h post injury (0.78 ± 12) ($n = 6$) vs. WT 10 pg/min ($^{\wedge}P = 0.001$); Tg 18 h post injury (0.76 ± 0.10) vs. Tg 10 pg/min (NS).

upregulates RGS4 in LDL receptor knockout mice. Dose infusion in their study was equivalent to 2480 pg/min in a 25 *g* mouse, which likely explains the blood pressure increase over this period of time from at least 108.0 ± 6.5(mm Hg) to 155.6 ± 11.6. Therefore, reported RGS4 levels after 4 weeks could not be uncoupled from a significant increase in systemic blood pressure and supraphysiologic dose of AngII.

We chose a model of 10 min unilateral injury (10UI) to highlight the anti-inflammatory potential of RGS4 in the absence of protracted ischemia and resultant tubular epithelial damage. In this model, AngII tissue levels 18 h after injury remained elevated 81.3% above sham levels. Low tubular injury scores and minimal KIM-1 expression indicated that tubular epithelial cell tissue quickly recovered from 10UI. Microvascular diameter as measured by intravital microscopy demonstrated a non-vasoconstricted state compared with controls, whereas dynamic MR studies showed blood flow to be reduced 18 h after 10UI. Pre-glomerular VSMCs were exposed to 1×10^{-9}mol/l AngII, which generated sufficient RANTES that could be measured in supernatant after 8 h. At equivalent AngII levels, RGS4 transgenic PGVSMC consistently expressed less RANTES compared with congenic controls. A change in blood flow by MR studies 18 h after reperfusion was therefore consistent with leukocyte localization in a setting absent of vasospasm. This parallels findings by Sanz and colleagues[14] who identified monocyte diapedesis at low AngII infusion rates, i.e. less than 100 ng/kg/min.[29] They observed monocytes adhering to mesenteric arterioles 4 h after an injection of 5.2 ng (approximately 17 ng/kg) of AngII in Sprague Dawley rats. At this dose mesenteric arteriolar diameter did not change. The same investigators demonstrated this with intravital microscopy using a 1 nmol/l infusion of AngII. When titrated, 100 nmol/l caused a 40% aggregate vascular collapse. However, the rate of infusion, and therefore ng/kg per unit time dose, was not clear from these studies.[32] Our *ex vivo* studies compared 40 pg/min with 10 pg/min with a notable change in vascular resistance at the higher dose. Our work does not identify the source of AngII during reperfusion injury, but it does emphasize that elevated levels of AngII are present for several hours after an ischemic insult.

We suggest that local AngII generation contributes to renal reperfusion injury in the kidney microvasculature by stimulating RANTES synthesis in VSMC. This signal appears

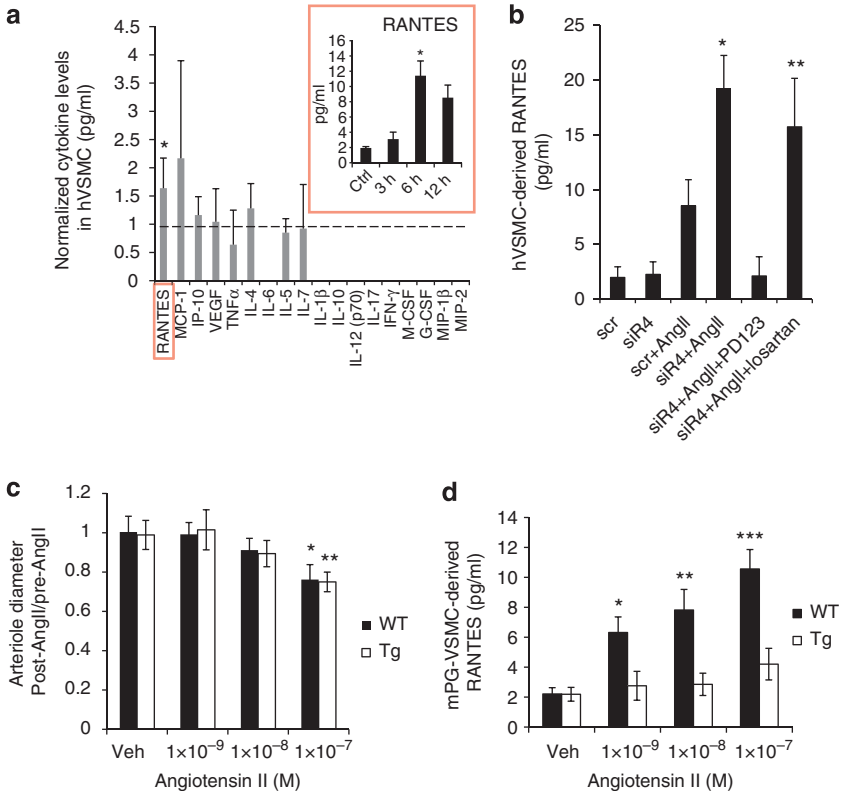

Figure 7 | Regulators of G protein signaling 4 (RGS4) inhibits vascular smooth muscle cells (VSMC)-derived regulated and normal t cell expressed and secreted (RANTES) expression after angiotensin-II (AngII) stimulation. (**a**) After AngII stimulation (100 nmol/l), human VSMC cytokine expression was analyzed by a Luminex-based assay containing microspheres specific to an array of cytokines (pg/ml): RANTES, MCP-1, IP-10, VEGF, TNFα, IL-4, IL-6, IL-5, IL-7, IL-1β, IL-10, IL-12 (p70), IL-17, IFN-γ, M-CSF, G-CSF, MIP-1β, and MIP-2. Each cytokine level from AngII-stimulated cells compared with vehicle (saline)-stimulated cells reported as a ratio. RANTES levels in stimulated cells ($n=8$) compared with unstimulated cells ($n=8$) were 1.56 ± 0.55 ($^{*}P<0.001$ by Student's *t*-test). Right inset (red box): 3, 6, and 12 h after AngII stimulation (10 nmol/m) compared with unstimulated controls. 3 h (3.10 ± 0.92) ($n=7$) vs. 6 h (11.41 ± 1.93) ($n=7$), ($^{*}P=8.3\times10^{-11}$). (**b**) RANTES expression after RGS4 inhibition and selective AngII receptor type 1 (AT1R) and AT2R inhibition. Scrambled siRNA (scr) + AngII (8.52 ± 2.39) ($n=6$) vs. RGS4-specific siRNA (siR4) (19.22 ± 3.03) ($n=6$),($^{*}P=1\times10^{-4}$); siR4 + AngII + PD123319 (2.51 ± 1.48) ($n=7$) vs. siR4 + AngII + losartan (15.73 ± 4.43) ($n=6$), ($^{**}P=2.6\times10^{-9}$). (**c**) Ratio of mouse-derived pre-glomerular arteriolar diameter post- compared with pre-AngII stimulation. Wild type (WT) + 1×10^{-8}M AngII (0.90 ± 0.04) ($n=5$) vs. WT + 1×10^{-7}M AngII (0.78 ± 0.09) ($n=5$), ($^{*}P=0.003$); transgenic (Tg) + 1×10^{-8}mol/l AngII (0.89 ± 0.07) vs. Tg + 1×10^{-7}mol/l AngII (0.75 ± 0.06), ($^{**}P=0.003$). (**d**) RANTES (pg/ml) levels in supernatant of pre-glomerular arteriole-derived (mouse) vs. zMC in culture after AngII stimulation. WT + 1×10^{-9}mol/l AngII (6.3 ± 1.0) ($n=5$) vs. Tg + 1×10^{-9}mol/l AngII (2.8 ± 1.0) ($n=5$), ($^{*}P=1.4\times10^{-6}$); WT + 1×10^{-8}mol/l AngII (7.8 ± 1.4) ($n=6$) vs. Tg + 1×10^{-8}mol/l AngII (2.9 ± 0.7) ($n=6$), ($^{**}P=1.2\times10^{-8}$); WT + 1×10^{-7}mol/l AngII (10.6 ± 1.3) ($n=6$) vs. Tg + 1×10^{-7}mol/l (4.2 ± 1.1) ($n=6$), ($^{***}P=8.2\times10^{-8}$) G-CSF, granulocyte-colony stimulating factor; IFN, interferon; IL, interleukin; M-CSF, macrophage colony-stimulating factor; MIP, macrophage inflammatory protein; TNF, tumor necrosis factor; VEGF, vascular endothelial growth factor.

to be initiated by AngII receptor type 2 activation. Despite the anti-inflammatory role attributed to AngII receptor type 2 activation, its role in renal pathology is well documented.[33,34] Only select cytokines are synthesized by VSMCs,[26] including RANTES, MCP-1, VEGF, and IL-8. We found one such cytokine, rRANTES, to be increased with AngII and more so in cells pretreated with RGS4 siRNA. RANTES is a chemokine found to have a central role in monocyte chemotaxis in the kidney[35] and the VSMC injury response.[36] RANTES has also been identified as an output to AngII stimulation in VSMCs.[37] However, we are the first to describe the AngII input leading to RANTES secretion by VSMCs, which can be manipulated by RGS4 expression. Treatment with AT_2-specific inhibitor, PD123319, in distinction to losartan, confirmed that RANTES expression was dependent on AT_2 receptor activation in isolated VSMCs. RGS4 knockdown experiments showed that AT_2 receptor signaling was modulated by RGS4. Wolf *et al.*[35] previously identified a kidney-derived RANTES response to AngII but focused on expression in glomerular endothelial cells.

RGS4 animal reporter models and *in vitro* interrogation were suggestive of RGS4 function derived from the VSMC. To investigate these findings further, we tested the function of a smooth muscle cell–specific RGS4 knockout under conditions of 10 min unilateral ischemia (10UI). We used an *in vivo* assay for macrophage localization to show that blood flow alterations seen in dynamic MR were due to leukocyte adhesion in a non-vasoconstricted period of reperfusion. We

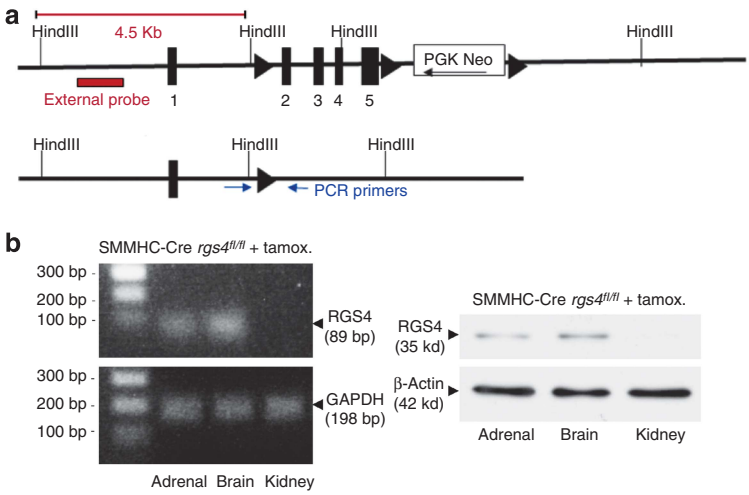

Figure 8 | Vascular smooth muscle cell–specific deletion of regulators of G protein signaling 4 (RGS4) in an animal model. (**a**) RGS4 floxed design, (**b**) (left) RGS4 transcript, and (right) RGS4 protein expression in the adrenal gland (zona glomerulosa cells), brain (neurons), and kidney (vascular smooth muscle cells) of SMMHC-Cre *rgs4*$^{fl/fl}$ animals after tamoxifen induction.

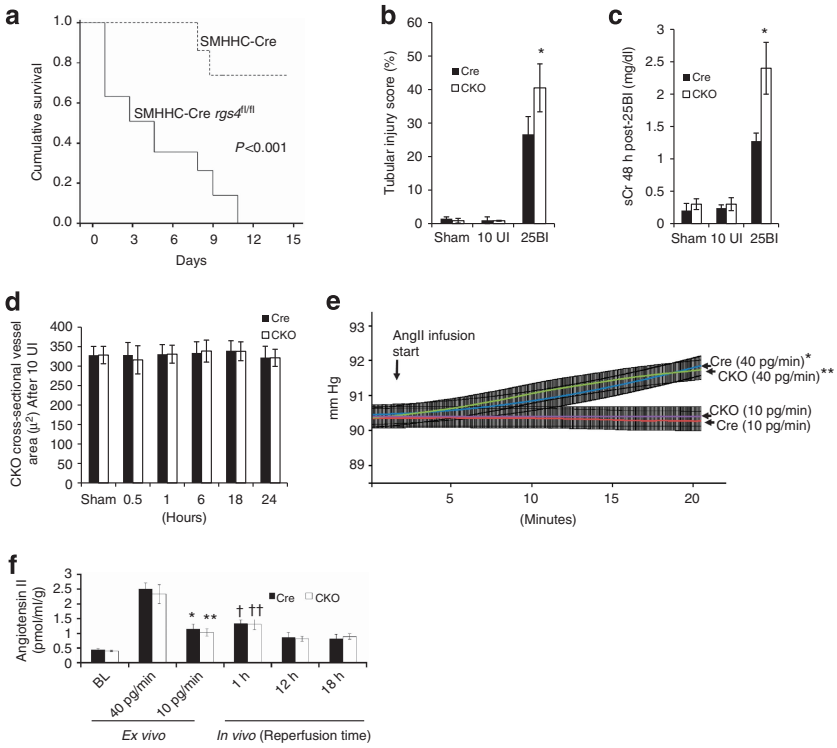

Figure 9 | SMMHC-Cre *rgs4*$^{fl/fl}$ response to ischemia/reperfusion injury. (**a**) Fourteen day survival in SMMHC-Cre controls (Cre) ($n=8$) and SMMHC-regulators of G protein signaling 4 (RGS4) knockout animals (CKO) ($n=8$) after 25 min bilateral renal ischemia (the Mantel–Cox log rank test $P<0.001$). (**b**) Tubular injury score after 24 h (Cre + 25 min bilateral ischemic injury (25BI) (926.7 ± 5.8%) ($n=7$) vs. CKO + 25BI (40.5 ± 4.9%) ($n=7$), $^{*}P=7.6\times10^{-7}$). (**c**) Serum creatinine after 48 h (Cre + 25BI (1.26 ± 0.13)($n=6$) vs. CKO + 25BI (1.92 ± 0.21) ($n=5$),$^{*}P=5.2\times10^{-7}$. (**d**) Vessel area after 10 min unilateral ischemia (10UI) in Cre and CKO at baseline (BL), 0.5, 1, 6, 18, and 24 h after microvascular clamp release. (**e**) Baseline Cre perfusion pressure 90.42 ± 0.35 ($n=6$) vs. 91.90 ± 0.39 ($n=6$) Cre after 20 min of angiotensin-II (AngII) infusion, 40 pg/min ($^{*}P=1.2\times10^{-7}$); baseline Cre vs. 20 min of AngII infusion, 10 pg/min, 90.36 ± 0.37 mm Hg ($n=6$) ($P=$ NS). Baseline CKO perfusion pressure 90.44 ± 0.37 ($n=6$) vs. 91.85 ± 0.38 ($n=6$) CKO after 20 min of AngII infusion, 40 pg/min ($^{**}P=2.7\times10^{-7}$); baseline CKO vs. 20 min of AngII infusion, 10 pg/min, 90.38 ± 0.35 mm Hg ($n=6$) ($P=$ NS). (**f**) AngII kidney tissue levels. Kidneys were isolated and infused with 40 pg/min, and 10 pg/min. Injured kidneys were procured after 1, 12, and 18 h of reperfusion subsequent to 10 min unilateral microvascular clamping. AngII kidney levels (pmol/ml per g of kidney) in Cre undergoing sham injury (0.45 ± 0.03) ($n=6$) vs. Cre 10 pg/min (1.15 ± 0.16) ($n=6$), ($^{*}P=1.1\times10^{-4}$); CKO BL (0.40 ± 0.02) ($n=6$) vs. CKO 10 pg/min (1.03 ± 0.12) ($n=6$), ($^{**}P=7.5\times10^{-4}$); Cre 40 pg/min (2.51 ± 0.21) ($n=6$) vs. Cre 1 h post injury (1.32 ± 0.12) ($n=6$), ($^{\dagger}1.26\times10^{-7}$); CKO 40 pg/min (2.33 ± 0.32) ($n=6$) vs. CKO 1 h post injury (1.31 ± 0.12) ($n=6$), ($^{\dagger\dagger}P=7.14\times10^{-7}$); Cre 18 h post injury (0.82 ± 0.15) ($n=6$) vs. Cre 10 pg/min (NS); CKO 18 h post injury (0.0.89 ± 0.10) ($n=6$) vs. CKO 10 pg/min (NS). NS, not significant; SMMHC, smooth muscle myosin heavy chain.

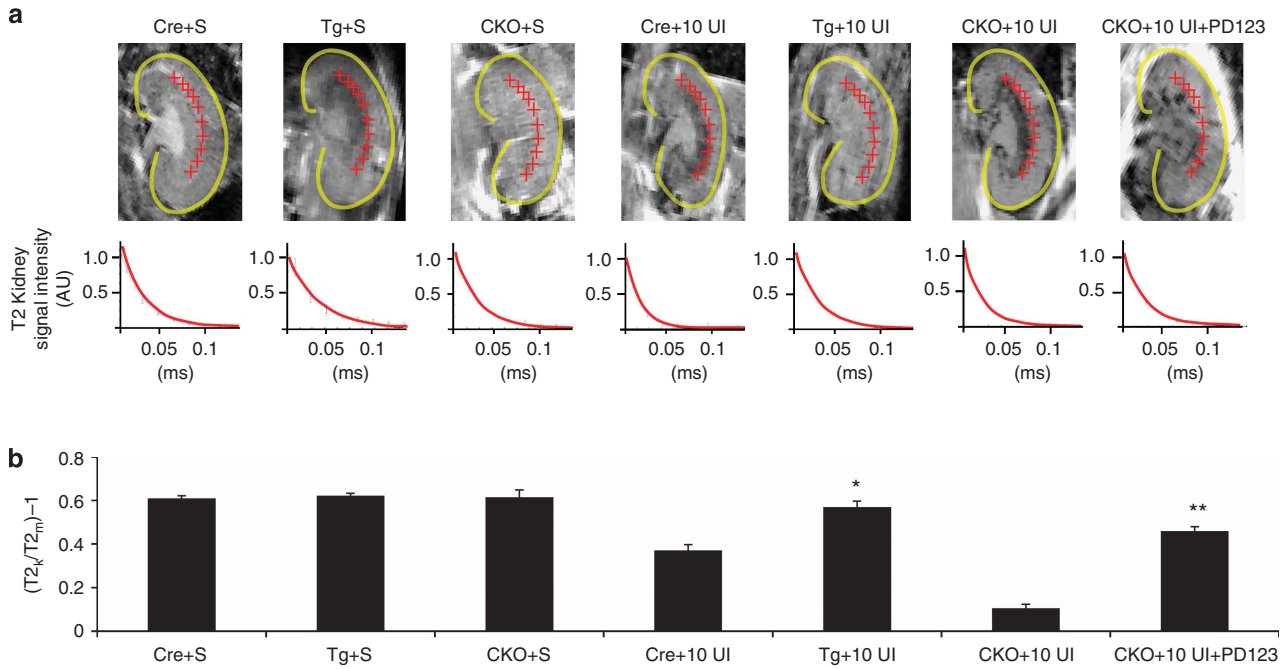

Figure 10 | T2 imaging of injured kidneys in the coronal plane 18 h after monocrystalline iron oxide nanoparticles -47 (MION-47) injection and 10 min unilateral ischemia injury. (**a**) SMMHC-Cre undergoing sham procedure (Cre + S), regulators of G protein signaling 4 (RGS4) overexpressor undergoing sham procedure transgenic (Tg + S), SMMHC-Cre *rgs4* null undergoing sham procedure (CKO + S), SMMHC-Cre undergoing 10 min unilateral ischemia (Cre + 10 min unilateral ischemia (10UI)), RGS4 overexpressor undergoing 10 min unilateral ischemia (Tg + 10UI), SMMHC-Cre *rgs4* null undergoing 10 min unilateral ischemia (CKO + 10UI), and SMMHC-Cre *rgs4* null treated with PD123319 undergoing 10 min unilateral ischemia (CKO + 10UI + PD123). (**b**) T2 signal decay curves were measured subsequent to 10 min microvascular clamping and 18 h of reperfusion. Regions of interest selected at the corticomedullary junction (red crosshairs). Calculated T2 signal in kidney ($T2_k$) was compared with calculated T2 signal in adjacent psoas muscle ($T2_m$). Cre + 10UI (0.37 ± 0.03) ($n = 7$) vs. TG + 10UI (0.57 ± 0.03) ($n = 7$) ($^*P = 1.2\times10^{-6}$); CKO + 10UI (0.11 ± 0.02) ($n = 7$) vs. CKO + 10UI + PD123319 (0.46 ± 0.02) ($n = 7$) ($^{**}P = 2.3\times10^{-8}$).

took advantage of macrophage avidity for the monocrystalline iron oxide particle, MION-47. Iron oxide nanoparticles have been used to localize this cell type noninvasively using T2-weighted MRI in the development of macrophage-driven insulitis.[31] Using this same technique we noninvasively showed an increase in macrophage density in the kidneys of conditional knockout animals 18 h after 10 min unilateral injury. This corresponded with elevated AngII tissue levels that did not induce vasoconstriction in isolated, perfused kidneys. Transgenic animals under the same 10UI conditions had a decrease in macrophage density compared with wild-type animals and more so compared with conditional knockout animals.

We did not investigate thromboxane A2, prostaglandin E2, bradykinin, or norepinephrine activity, although these receptors incorporate the Gα subunit and have been implicated in the pathophysiology of IRI. Work by Snoeijs [38]*et al.* described little evidence that thromboxane A2 receptor knockout animals are less susceptible to IRI. Prostaglandin E2 activity in respiratory epithelia appears to be moderated by RGS4;[39] however, endogenous expression of RGS4 in respiratory tubular epithelial cells is inconsistent with the cell type identified by the *rgs4* LacZ animal reporter model.[40] Bradykinin is known to mitigate ischemia/reperfusion injury;[41] however, the bradykinin 2 receptor–dependent signaling does not appear to be modulated by RGS4.[42] Norepinephrine is generated during renal ischemic injury; however, RANTES induction and/or resultant macrophage chemotaxis have not been reported as effectors. Further, AngII stimulation has been implicated in soluble guanylyl cyclase inhibition and myosin light chain kinase activation with a common result of blood flow reduction. Such studies rely on the vasoconstrictive effect of AngII, whereas we have tried to show that AngII can modulate blood flow independent of vessel diameter.

In our report, enhanced endogenous RGS4 expression was not durable after 12 h of reperfusion. This left the renal vasculature exposed to cell signaling effects of ligands such as AngII. We demonstrated this expression pattern in β-gal-expressing animals and confirmed these findings with localization of monoclonal antibodies against RGS4 in wild-type animals. Enhanced RGS4 expression in transgenic animals most likely offered the greatest protection during the first 12 h of reperfusion. This coincides with the nascent stages of the inflammatory response. In contrast, tissue in wild-type animals was exposed to prolonged G protein–coupled receptor signaling over the same time period. As a result, the wild-type animal model and the genetically deficient RGS4 animals were both more susceptible to reperfusion injury compared with the transgenic overexpressor. Partial recovery was shown in conditional knockouts treated with an Ang-II receptor type 2 antagonist. PPAR δ agonists have also been shown to upregulate RGS4 expression and

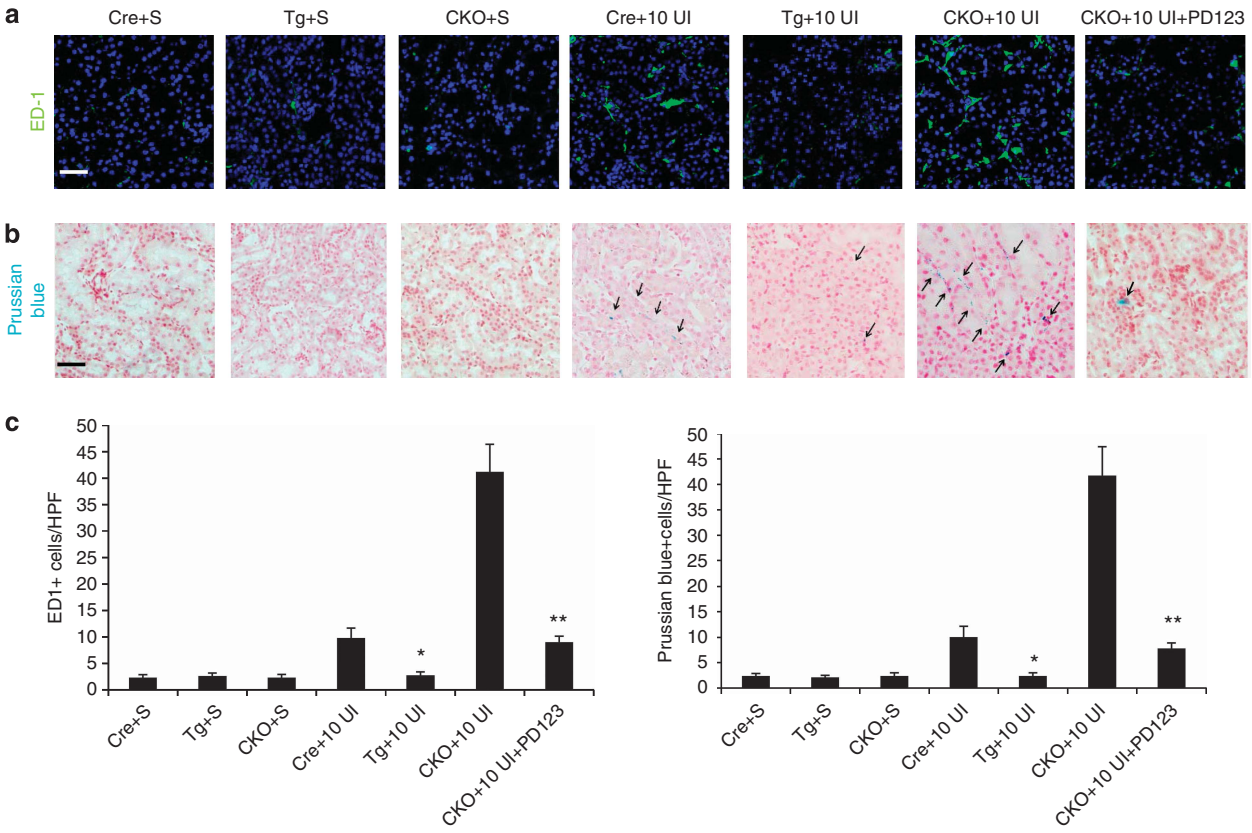

Figure 11 | Histologic analysis of kidneys subsequent to 10 min unilateral ischemia and monocrystalline iron oxide nanoparticles -47 (MION-47) injection and 18 h of reperfusion. (**a**,**c**) ED-1-positive cells (FITC) in SMMHC-Cre undergoing sham procedure (Cre + S), regulators of G protein signaling 4 (RGS4) overexpressor undergoing sham procedure transgenic (Tg + S), SMMHC-Cre *rgs4* null undergoing sham procedure (CKO + S), SMMHC-Cre undergoing 10 min unilateral ischemia (Cre + 10UI), RGS4 overexpressor undergoing 10 min unilateral ischemia (Tg + 10UI), SMMHC-Cre *rgs4* null undergoing 10 min unilateral ischemia (CKO + 10UI), and SMMHC-Cre *rgs4* null treated with PD123319 undergoing 10 min unilateral ischemia (CKO + 10UI + PD123). Cre + 10UI (10 ± 2 cells) ($n = 10$) vs. Tg + 10UI (3 ± 1) ($n = 10$) ($^{*}P = 1.1\times10^{-8}$); (CKO + 10UI) (41 ± 5) ($n = 10$) vs. (CKO + 10UI + PD123) (9 ± 1) ($n = 10$) ($^{**}P = 1.0\times10^{-10}$). Scale bar = 50 μm (**b**,**c**) Prussian blue staining of above tissue (scale bar = 50 μm). Cre + 10UI (10 ± 2 cells) ($n = 10$) vs. Tg + 10UI (4 ± 1) ($n = 10$) ($^{*}P = 2.1\times10^{-8}$); (CKO + 10UI) (42 ± 6) ($n = 10$) vs. (CKO + 10UI + PD123) (8 ± 1) ($n = 10$) ($^{**}P = 3.2\times10^{-11}$) (Scale bar = 50 μm).

inhibit atherosclerotic plaque development.[3] PPAR δ agonists may be protective in kidney reperfusion injury but have not yet been investigated in this model. Such targeted therapies are desirable to avoid the relative contraindication of Ang-II receptor type 1 antagonists for the treatment of ischemia/reperfusion injury.

In conclusion G protein–coupled receptor signaling is modulated by RGS4 in two conditions of acute kidney injury: (1) early ischemia and (2) extended reperfusion. During reperfusion injury, RGS4 resists AngII receptor signaling in VSMCs, thereby preventing the influx of macrophages triggered by cytokine release and cell damage (Figure 12). Our studies bring to focus both the receptor–ligand interaction and the cell type critical in the pathophysiology of nascent reperfusion injury.

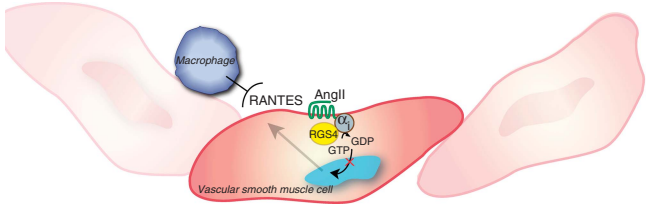

Figure 12 | Regulators of G protein signaling 4 (RGS4) function in kidney smooth muscle cells. During kidney reperfusion, RGS4 dampens angiotensin II-induced regulated and normal t cell expressed and secreted (RANTES) generation in vascular smooth muscle cells, which is in turn responsible for macrophage localization and endothelial injury.

Statistical techniques

Sigmastat v3.1 (Systat Software, San Jose, CA) software was used to calculate all statistics. Experimental conditions were evaluated for significance using analysis of variance for pair-wise comparison among multiple groups using the Holm–Sidak method for multiple comparisons. Student's *t*-test was used to evaluate for significance between two groups. One-way analysis of variance calculations were used for all comparisons unless otherwise stated in the text. Log-rank testing (Mantel–Cox) was used to compare survival

between two groups. All values represent a condition's mean value ± standard deviation.

MATERIALS AND METHODS

Serum creatinine and Urea measurements

Serum creatinine measurement was analyzed by high-performance liquid chromatography at the University of Alabama in Birmingham core facility for Acute Kidney Injury Research as previously described.[43] The Urea Fluorometric Assay Kit (Cayman Chemical, Ann Arbor, MI) was used as per the manufacturer's recommendations.

Multiphoton intra-vital microscopy

Animals underwent IRI and then were secured and interrogated on a multiphoton microscope platform (Bruker, The Woodlands, TX).

AngII immunoassay

AngII Immunoassay (Cayman Chemical) was used to determine tissue Ang-II concentrations according to the manufacturer's instructions.

Dynamic magnetic resonance imaging

Data acquisition was processed using TopSpin 3.1 software (Bruker Biospin, The Woodlands, TX). All post-acquisition analysis was performed with Bayesian Analysis Software (Washington University, St Louis, MO, USA).

Flow cytometry

Cells were collected and digested in collagenase in a 37 °C water bath for 30 min and permeabilized for analysis on a BD Accuri C6 flow cytometer (BD Biosciences, Franklin Lakes, NJ).

Ex vivo kidney perfusion

Isolated kidneys were analyzed using a programmable peristaltic pump and in-line pressure monitor.

Human vascular smooth muscle cell culture

Cells were obtained (Sciencell) and cultured in VSMC media (Sciencell, Carlsbad, CA).

Pre-glomerular vascular smooth muscle cell culture

Kidney tissue was isolated following the technique of Dubey *et al.*.[27]

CCL5/RANTES immunoassay

The enzyme-linked immune sorbent assay-based assay kit (R&D Systems, Minneapolis, MN) was used following the manufacturer's specifications.

Magnetic microsphere-assisted cytokine immunoassay

Adult VSMCs (Sciencell) were processed. The multi-analyte microsphere-based fluorometric assay was performed using the Luminex technology (Luminex, Austin, TX) under the manufacturer's specifications.

SMMHC-Cre x RGS4 flox design

The gene targeting vector included a neomycin resistance cassette to select for screened embryonic stem cells incorporating the target sequence. *RGS4 flox*–expressing animals were then crossed with *SMMHC-Cre*–expressing for 10 generations.

In vivo imaging of monocrystalline nanoparticles

T2 signal decay patterns were generated using rapid acquisition with relaxation enhancement with variable repetition time [RAREVTR] protocol.

DISCLOSURE

All the authors declared no competing interests.

ACKNOWLEDGMENTS

This work was supported by NIH grants R01 HL061567 (AJM), P30 DK079333 (AMS and AJM), K08DK089002 (AMS), R37DK039773 (JVB), RO1AI069259 (UHvA) and PO1AI078897 (UHvA), UAB/UCSD 'Brien Core Center for Acute Kidney Injury Research (NIH P30 DK 079337), and a Shared Instrumentation Grant S10 RR028792 at Beth Israel Deaconess Medical Center.

SUPPLEMENTARY MATERIAL

Supplementary material is linked to the online version of the paper at http://www.nature.com/ki

REFERENCES

1. Gurley SB, Griffiths RC, Mendelsohn ME *et al.* Renal actions of RGS2 control blood pressure. *J Am Soc Nephrol* 2010; **21**: 1847–1851.
2. Siedlecki AM, Jin X, Thomas W *et al.* RGS4, a GTPase activator, improves renal function in ischemia-reperfusion injury. *Kidney Int* 2011; **80**: 263–271.
3. Takata Y, Liu J, Yin F *et al.* PPARdelta-mediated antiinflammatory mechanisms inhibit angiotensin II-accelerated atherosclerosis. *Proc Natl Acad Sci USA* 2008; **105**: 4277–4282.
4. Barish GD, Atkins AR, Downes M *et al.* PPARdelta regulates multiple proinflammatory pathways to suppress atherosclerosis. *Proc Natl Acad Sci USA* 2008; **105**: 4271–4276.
5. Harris IS, Treskov I, Rowley MW *et al.* G-protein signaling participates in the development of diabetic cardiomyopathy. *Diabetes* 2004; **53**: 3082–3090.
6. Heximer SP, Blumer KJ. RGS proteins: Swiss army knives in seven-transmembrane domain receptor signaling networks. *Sci STKE* 2007; **2007*pe2*.**
7. Cifelli C, Rose RA, Zhang H *et al.* RGS4 regulates parasympathetic signaling and heart rate control in the sinoatrial node. *CirRes* 2008; **103**: 527–535.
8. Zarzuelo MJ, Jimenez R, Galindo P *et al.* Antihypertensive effects of peroxisome proliferator-activated receptor-beta activation in spontaneously hypertensive rats. *Hypertension* 2011; **58**: 733–743.
9. Kleemann P, Papa D, Vigil-Cruz S *et al.* Functional reconstitution of the human chemokine receptor CXCR4 with G(i)/G (o)-proteins in Sf9 insect cells. *Naunyn-Schmiedeberg's ArchPharmacol* 2008; **378**: 261–274.
10. Tamirisa P, Blumer KJ, Muslin AJ. RGS4 inhibits G-protein signaling in cardiomyocytes. *Circulation* 1999; **99**: 441–447.
11. Sprague AH, Khalil RA. Inflammatory cytokines in vascular dysfunction and vascular disease. *Biochem Pharmacol* 2009; **78**: 539–552.
12. Chen J, Chen JK, Nagai K *et al.* EGFR signaling promotes TGFbeta-dependent renal fibrosis. *J Am SocNephrol* 2012; **23**: 215–224.
13. Adams GN, LaRusch GA, Stavrou E *et al.* Murine prolylcarboxypeptidase depletion induces vascular dysfunction with hypertension and faster arterial thrombosis. *Blood* 2011; **117**: 3929–3937.
14. Alvarez A, Cerda-Nicolas M, Naim Abu Nabah Y *et al.* Direct evidence of leukocyte adhesion in arterioles by angiotensin II. *Blood* 2004; **104**: 402–408.
15. Zhou Z, Hu CP, Wang CJ *et al.* Calcitonin gene-related peptide inhibits angiotensin II-induced endothelial progenitor cells senescence through up-regulation of klotho expression. *Atherosclerosis* 2010; **213**: 92–101.
16. Bonventre JV, Yang L. Cellular pathophysiology of ischemic acute kidney injury. *J Clin Invest* 2011; **121**: 4210–4221.
17. Wilhelm SM, Simonson MS, Robinson AV *et al.* Endothelin up-regulation and localization following renal ischemia and reperfusion. *Kidney Int* 1999; **55**: 1011–1018.

18. Arendshorst WJ, Brannstrom K, Ruan X. Actions of angiotensin II on the renal microvasculature. *J Am Soc Nephrol* 1999; **10**(Suppl 11): S149–S161.
19. Gulmen S, Kiris I, Narin C *et al.* Tezosentan reduces the renal injury induced by abdominal aortic ischemia-reperfusion in rats. *J Surg Res* 2009; **157**: e7–e13.
20. Danilov SM, Sadovnikova E, Scharenborg N *et al.* Angiotensin-converting enzyme (CD143) is abundantly expressed by dendritic cells and discriminates human monocyte-derived dendritic cells from acute myeloid leukemia-derived dendritic cells. *Exp Hematol* 2003; **31**: 1301–1309.
21. Komine N, Khang S, Wead LM *et al.* Effect of combining an ACE inhibitor and an angiotensin II receptor blocker on plasma and kidney tissue angiotensin II levels. *Am J Kidney Dis* 2002; **39**: 159–164.
22. Ding J, Guzman JN, Tkatch T *et al.* RGS4-dependent attenuation of M4 autoreceptor function in striatal cholinergic interneurons following dopamine depletion. *Nat Neurosci* 2006; **9**: 832–842.
23. Winden KD, Oldham MC, Mirnics K *et al.* The organization of the transcriptional network in specific neuronal classes. *Mol Syst Biol* 2009; **5**: 291.
24. Siedlecki A, Anderson JR, Jin X *et al.* RGS4 controls renal blood flow and inhibits cyclosporine-mediated nephrotoxicity. *Am J Transplant* 2010; **10**: 231–241.
25. Lee JJ, Bretthorst GL, Derdeyn CP *et al.* Dynamic susceptibility contrast MRI with localized arterial input functions. *Magn Reson Med* 2010; **63**: 1305–1314.
26. Jordan NJ, Watson ML, Williams RJ *et al.* Chemokine production by human vascular smooth muscle cells: modulation by IL-13. *Br J Pharmacol* 1997; **122**: 749–757.
27. Dubey RK, Roy A, Overbeck HW. Culture of renal arteriolar smooth muscle cells. Mitogenic responses to angiotensin II. *Circ Res* 1992; **71**: 1143–1152.
28. Wirth A, Benyo Z, Lukasova M *et al.* G12-G13-LARG-mediated signaling in vascular smooth muscle is required for salt-induced hypertension. *Nat Med* 2008; **14**: 64–68.
29. Basile DP, Leonard EC, Beal AG *et al.* Persistent oxidative stress following renal ischemia-reperfusion injury increases ANG II hemodynamic and fibrotic activity. *Am J Physiol Renal Physiol* 2012; **302**: F1494–F1502.
30. Rovner AS, Murphy RA, Owens GK. Expression of smooth muscle and nonmuscle myosin heavy chains in cultured vascular smooth muscle cells. *J Biol Chem* 1986; **261**: 14740–14745.
31. Fu W, Wojtkiewicz G, Weissleder R *et al.* Early window of diabetes determinism in NOD mice, dependent on the complement receptor CRIg, identified by noninvasive imaging. *Nat Immunol* 2012; **13**: 361–368.
32. Piqueras L, Kubes P, Alvarez A *et al.* Angiotensin II induces leukocyte-endothelial cell interactions in vivo via AT(1) and AT(2) receptor-mediated P-selectin upregulation. *Circulation* 2000; **102**: 2118–2123.
33. Esteban V, Lorenzo O, Ruperez M *et al.* Angiotensin II, via AT1 and AT2 receptors and NF-kappaB pathway, regulates the inflammatory response in unilateral ureteral obstruction. *J Am Soc Nephrol* 2004; **15**: 1514–1529.
34. Wolf G, Wenzel U, Burns KD *et al.* Angiotensin II activates nuclear transcription factor-kappaB through AT1 and AT2 receptors. *Kidney Int* 2002; **61**: 1986–1995.
35. Wolf G, Ziyadeh FN, Thaiss F *et al.* Angiotensin II stimulates expression of the chemokine RANTES in rat glomerular endothelial cells. Role of the angiotensin type 2 receptor. *J Clin Invest* 1997; **100**: 1047–1058.
36. Ullevig S, Zhao Q, Lee CF *et al.* NADPH oxidase 4 mediates monocyte priming and accelerated chemotaxis induced by metabolic stress. *Arterioscler Thromb Vasc Biol* 2012; **32**: 415–426.
37. Guzik TJ, Hoch NE, Brown KA *et al.* Role of the T cell in the genesis of angiotensin II induced hypertension and vascular dysfunction. *J Exp Med* 2007; **204**: 2449–2460.
38. Snoeijs MG, Hoogland PR, Boonen B *et al.* Thromboxane receptor signalling in renal ischemia reperfusion injury. *Free Radic Res* 2011; **45**: 699–706.
39. Song KS, Choi YH, Kim JM *et al.* Suppression of prostaglandin E2-induced MUC5AC overproduction by RGS4 in the airway. *American J Physiol Lung Cell Mol Physiol* 2009; **296**: L684–L692.
40. Eppig JT, Blake JA, Bult CJ *et al.* The Mouse Genome Database (MGD): comprehensive resource for genetics and genomics of the laboratory mouse. *Nucleic Acids Res* 2012; **40**(Database issue): D881–D886.
41. Kakoki M, McGarrah RW, Kim HS *et al.* Bradykinin B1 and B2 receptors both have protective roles in renal ischemia/reperfusion injury. *Proc Natl Acad Sci USA* 2007; **104**: 7576–7581.
42. Wang Q, Traynor JR. Opioid-induced down-regulation of RGS4: role of ubiquitination and implications for receptor cross-talk. *J Biol Chem* 2011; **286**: 7854–7864.
43. Young S, Struys E, Wood T. Quantification of creatine and guanidinoacetate using GC-MS and LC-MS/MS for the detection of cerebral creatine deficiency syndromes. *Cur Protoc Hum Genet* 2007; **Chapter 17**: Unit 17 13.